The Photon Collider

at TESLA

V. Telnov

INP, Novosibirsk and DESY

(Reviev of the TDR)

1 The Photon Collider at TESLA

B. Badelek[43], C. Blöchinger[44], J. Blümlein[12], E. Boos[28], R. Brinkmann[12], H. Burkhardt[11], P. Bussey[17], C. Carimalo[33], J. Chyla[34], A.K. Çiftçi[4], W. Decking[12], A. De Roeck[11], V. Fadin[10], M. Ferrario[15], A. Finch[24], H. Fraas[44], F. Franke[44], M. Galynskii[27], A. Gamp[12], I. Ginzburg[31], R. Godbole[6], D.S. Gorbunov[28], G. Gounaris[39], K. Hagiwara[22], L. Han[19], R.-D. Heuer[18], C. Heusch[36], J. Illana[12], V. Ilyin[28], P. Jankowski[43], Yi Jiang[19], G. Jikia[16], L. Jönsson[26], M. Kalachnikow[8], F. Kapusta[33], R. Klanner[12,18], M. Klasen[12], K. Kobayashi[41], T. Kon[40], G. Kotkin[30], M. Krämer[14], M. Krawczyk[43], Y.P. Kuang[7], E. Kuraev[13], J. Kwiecinski[23], M. Leenen[12], M. Levchuk[27], W.F. Ma[19], H. Martyn[1], T. Mayer[44], M. Melles[35], D.J Miller[25], S. Mtingwa[29], M. Mühlleitner[12], B. Muryn[23], P.V. Nickles[8], R. Orava[20], C. Pancheri[15], A. Penin[12], A. Potylitsyn[42], P. Poulose[6], T. Quast[8], P. Raimondi[37], H. Redlin[8], F. Richard[32], S.D. Rindani[2], T. Rizzo[37], E. Saldin[12], W. Sandner[8], H. Schönnagel[8], E. Schneidmiller[12], H.J. Schreiber[12], S. Schreiber[12], K.P. Schüler[12], V. Serbo[30], A. Seryi[37], R. Shanidze[38], W. da Silva[33], S. Söldner-Rembold[11], M. Spira[35], A.M. Stasto[23], S. Sultansoy[5], T. Takahashi[21], V. Telnov[10,12], A. Tkabladze[12], D. Trines[12], A. Undrus[9], A. Wagner[12], N. Walker[12], I. Watanabe[3], T. Wengler[11], I. Will[8,12], S. Wipf[12], Ö. Yavaş[4], K. Yokoya[22], M. Yurkov[12], A.F. Zarnecki[43], P. Zerwas[12], F. Zomer[32].

[1] RWTH Aachen, Germany
[2] PRL, Ahmedabad, India
[3] Akita KeizaiHoka University, Japan
[4] Ankara University, Turkey
[5] Gazi University, Ankara, Turkey
[6] Indian Institute of Science, Bangalore, India
[7] Tsinghua University, Beijing, P.R. China
[8] Max–Born–Institute, Berlin, Germany
[9] BNL, Upton, USA
[10] Budker INP, Novosibirsk, Russia
[11] CERN, Geneva, Switzerland
[12] DESY, Hamburg and Zeuthen, Germany
[13] JINR, Dubna, Russia
[14] University of Edinburgh, UK
[15] INFN-LNF, Frascati, Italy
[16] Universität Freiburg, Germany
[17] University of Glasgow, UK
[18] Universität Hamburg, Germany
[19] CUST, Hefei, P.R.China
[20] University of Helsinki, Finland
[21] Hiroshima University, Japan
[22] KEK, Tsukuba, Japan
[23] INP, Krakow, Poland
[24] University of Lancaster, UK
[25] UCL, London, UK
[26] University of Lund, Sweden
[27] Inst. of Physics, Minsk, Belarus
[28] Moscow State University, Russia
[29] N.Carolina Univ., USA
[30] Novosibirsk State University, Russia
[31] Inst. of Math., Novosibirsk, Russia
[32] LAL, Orsay, France
[33] Université de Paris VI–VII, France
[34] IP, Prague, Czech Republic
[35] PSI, Villingen, Switzerland
[36] UCSC, Santa Cruz, USA
[37] SLAC, Stanford, USA
[38] Tbilisi State University, Georgia
[39] University of Thessaloniki, Greece
[40] Seikei University, Tokyo, Japan
[41] Sumimoto Heavy Industries, Tokyo, Japan
[42] Polytechnic Institute, Tomsk, Russia
[43] Warsaw University, Poland
[44] Universität Würzburg, Germany

Contents

Scheme of $\gamma\gamma$, γe collider

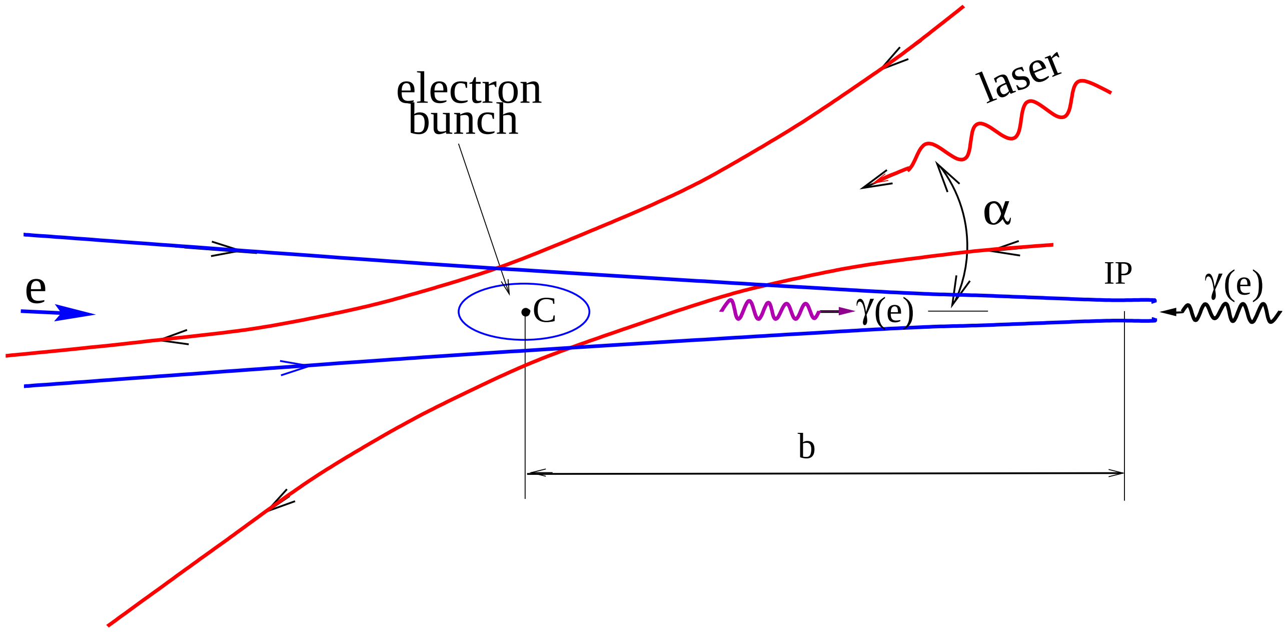

a)

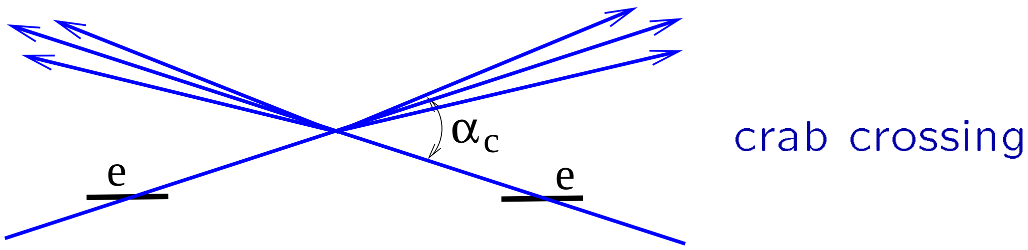

b)

$$\omega_m = \frac{x}{x+1}E_0; \quad x \approx \frac{4E_0\omega_0}{m^2c^4} \simeq 15.3 \left[\frac{E_0}{\mathrm{TeV}}\right]\left[\frac{\omega_0}{\mathrm{eV}}\right]$$

$E_0 = 250$ GeV, $\omega_0 = 1.17$ eV ($\lambda = 1.06$ μm) $\Rightarrow x = 4.5$ and $\omega_m = 0.82E_0 = 205$ GeV

Energy and luminosity of $\gamma\gamma$,γe collider based on TESLA

$2E_0$ (GeV)	200	500	800
$L_{geom}, 10^{34}$	4.8	12.0	19.1
$W_{\gamma\gamma,max}$ (GeV)	122	390	670
$L_{\gamma\gamma}(z > 0.8 z_{m,\gamma\gamma}), 10^{34}$	0.43	1.1	1.7
$W_{\gamma e,max}$ (GeV)	156	440	732
$L_{e\gamma}(z > 0.8 z_{m,\gamma e}), 10^{34}$	0.36	0.94	1.3
$L_{e^+e^-}, 10^{34}$	1.3	3.4	5.8

$$L_{\gamma\gamma}(z > 0.8 z_m) \sim \frac{1}{3} L_{e^+e^-}.$$

$$(z = W_{\gamma\gamma}/2E_0)$$

Typical cross sections in $\gamma\gamma$, γe and e^+e^- collisions.

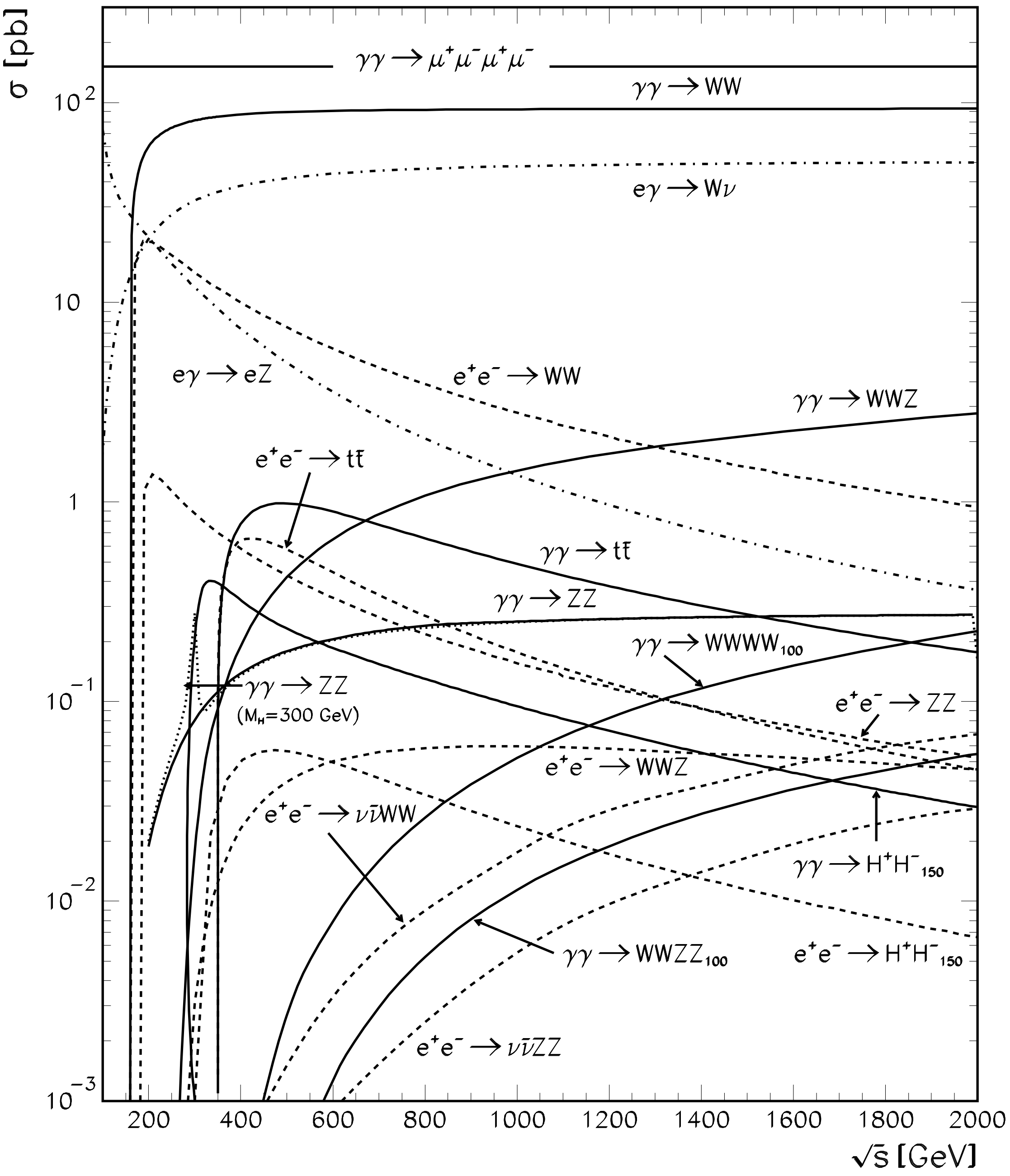

Charged pair production in e^+e^- and $\gamma\gamma$ collisions.

(S (scalars), F (fermions), W (W-bosons);
$\sigma = (\pi\alpha^2/M^2) f(x)$, beams unpolarized)

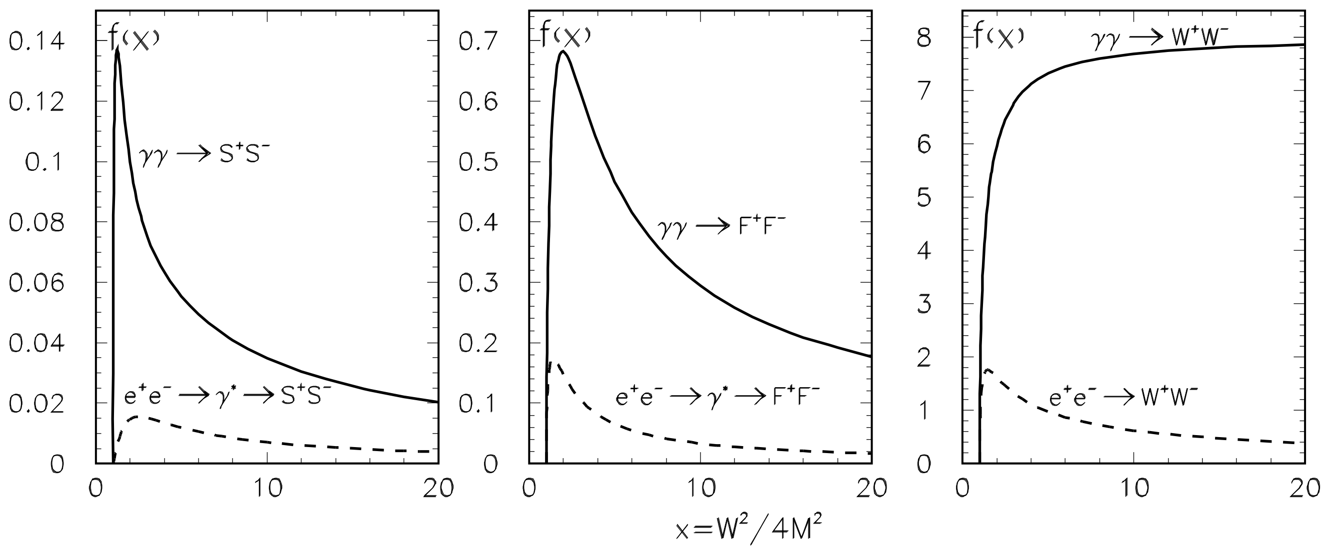

Cross sections for charged scalars, $2E_0 = 1$ TeV

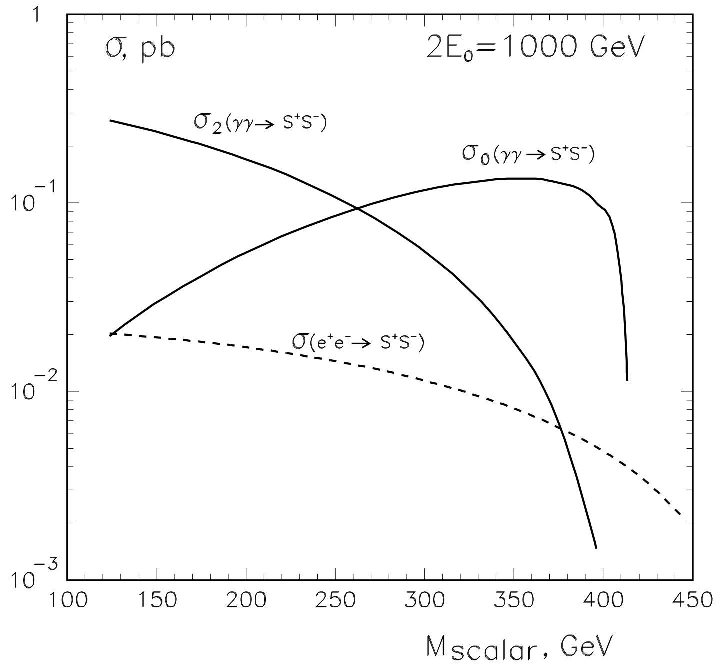

Cross sections of the Higgs boson production in $\gamma\gamma$ and e^+e^- collisions

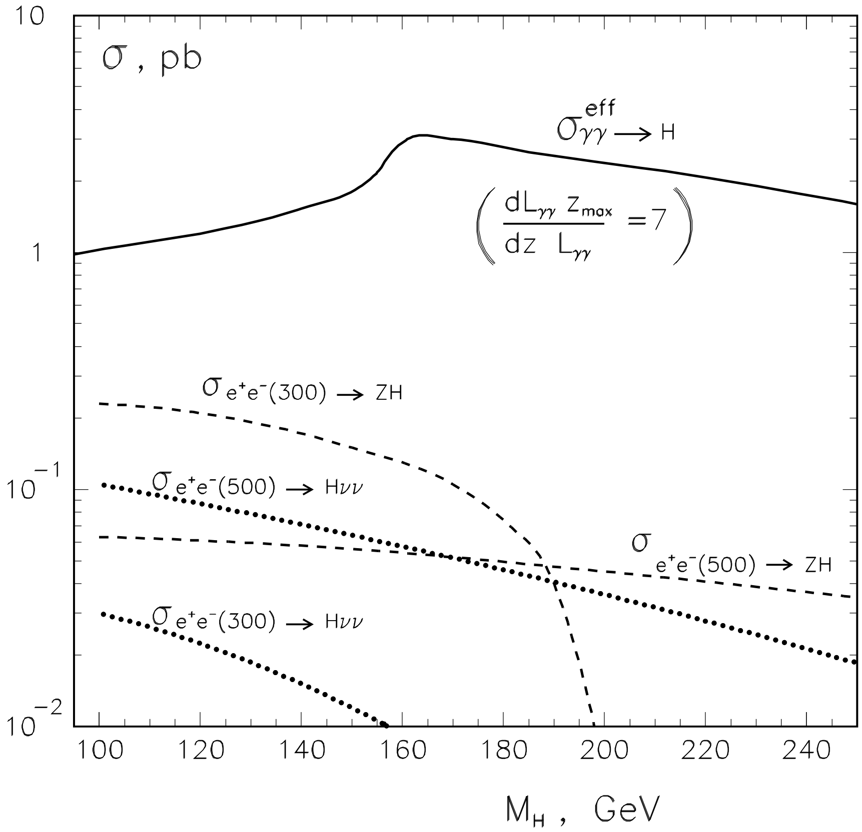

$$\dot{N}_{\gamma\gamma \to h} = L_{\gamma\gamma} \times \frac{dL_{\gamma\gamma} M_h}{dW_{\gamma\gamma} L_{\gamma\gamma}} \frac{4\pi^2 \Gamma_{\gamma\gamma}(1 + \lambda_1 \lambda_2)}{M_h^3} \equiv L_{\gamma\gamma} \times \sigma^{eff}$$

Higgs signal and heavy quark background for $M_h = 120$ GeV

(Soldner-Rembold, Jikia)

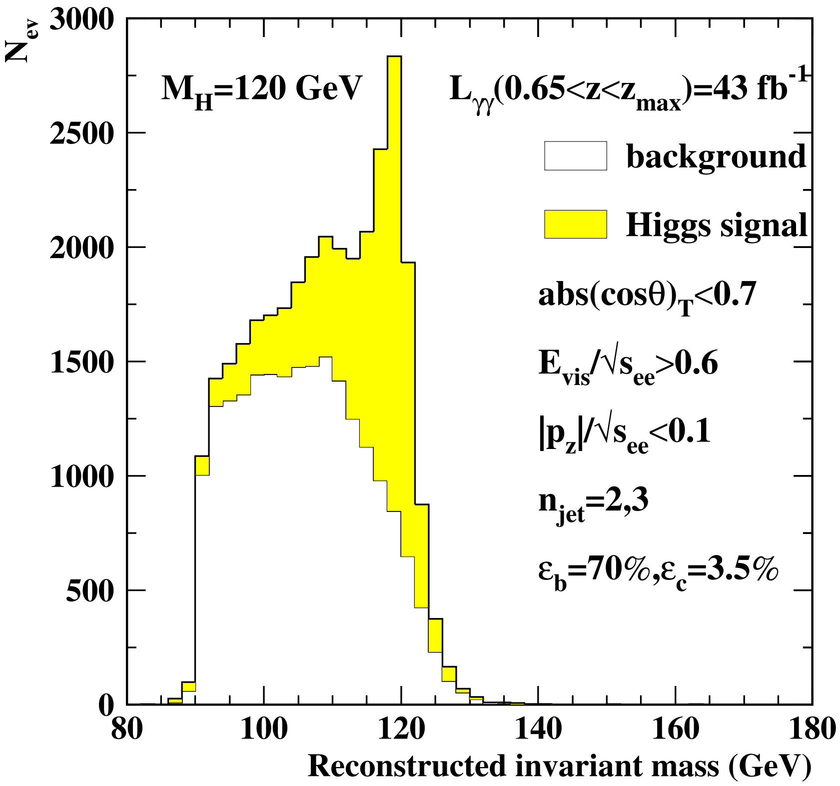

$$\frac{\Delta[\Gamma(h \to \gamma\gamma)BR(h \to \bar{b}b)]}{[\Gamma(h \to \gamma\gamma)BR(h \to \bar{b}b)]} \approx 2\%$$

Resonant heavy Higgs boson (H, A) production in $\gamma\gamma$ collisions with decay into $b\bar{b}$ pairs

(Mühleitner, Krämer, Spira, Zerwas)

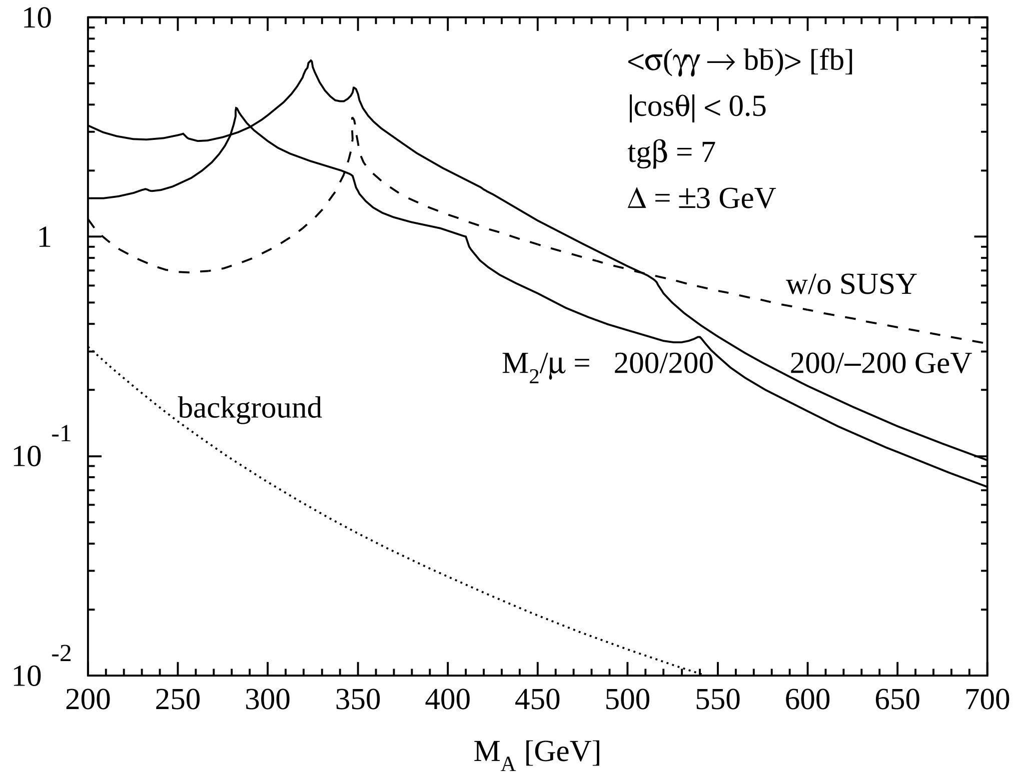

Note:

$M_H \approx M_A$, in e$^+$e$^-$ collisions H and A are produced in pairs, therefore

in e$^+$e$^-$ collisions $M_{H,A}^{max} \sim E_0$

in $\gamma\gamma$ collisions $M_{H,A}^{max} \sim 1.6 E_0$

Measurement of the Higgs CP properties

$$\sigma \propto 1 \pm l_{\gamma 1} l_{\gamma 2} \cos 2\phi,$$

where $l_{\gamma i}$ are the degrees of linear polarization and ϕ is the angle between $\vec{l_{\gamma 1}}$ and $\vec{l_{\gamma 2}}$, and the $\pm$ signs correspond to CP$= \pm 1$ scalar particles.

Measurement of CP violating asymmetry

$$\mathcal{A}_1 = \frac{|\mathcal{M}_{++}|^2 - |\mathcal{M}_{--}|^2}{|\mathcal{M}_{++}|^2 + |\mathcal{M}_{--}|^2}, \quad \mathcal{A}_2 = \frac{2Im(\mathcal{M}^*_{--}\mathcal{M}_{++})}{|\mathcal{M}_{++}|^2 + |\mathcal{M}_{--}|^2}.$$

$$T_- = \frac{N_{++} - N_{--}}{N_{++} + N_{--}} = \frac{\langle \xi_2 \rangle + \langle \tilde{\xi}_2 \rangle}{1 + \langle \xi_2 \tilde{\xi}_2 \rangle} \mathcal{A}_1,$$

$$T_\psi = \frac{N(\phi = \frac{\pi}{4}) - N(\phi = -\frac{\pi}{4})}{N(\phi = \frac{\pi}{4}) + N(\phi = -\frac{\pi}{4})} = \frac{\langle \xi_3 \tilde{\xi}_1 \rangle + \langle \xi_1 \tilde{\xi}_3 \rangle}{1 + \langle \xi_2 \tilde{\xi}_2 \rangle} \mathcal{A}_2,$$

Supersymmetry

A $\gamma\gamma$ collider can produce pairs of any charged particles (charged Higgs, supersymmetric particles etc.) with a cross section about one order of magnitude higher than those in e^+e^- collisions. Moreover, the cross sections depend differently on various physical parameters.

At a γe collider charged particles with masses higher than in e^+e^- collisions at the same collider can be produced (a heavy charged particle plus a light neutral one, such as a new W boson and neutrino or supersymmetric charged particle plus neutralino):

$$m_{\tilde{e}^-} < 0.9 \times 2E_0 - m_{\tilde{\chi}_1^0}$$

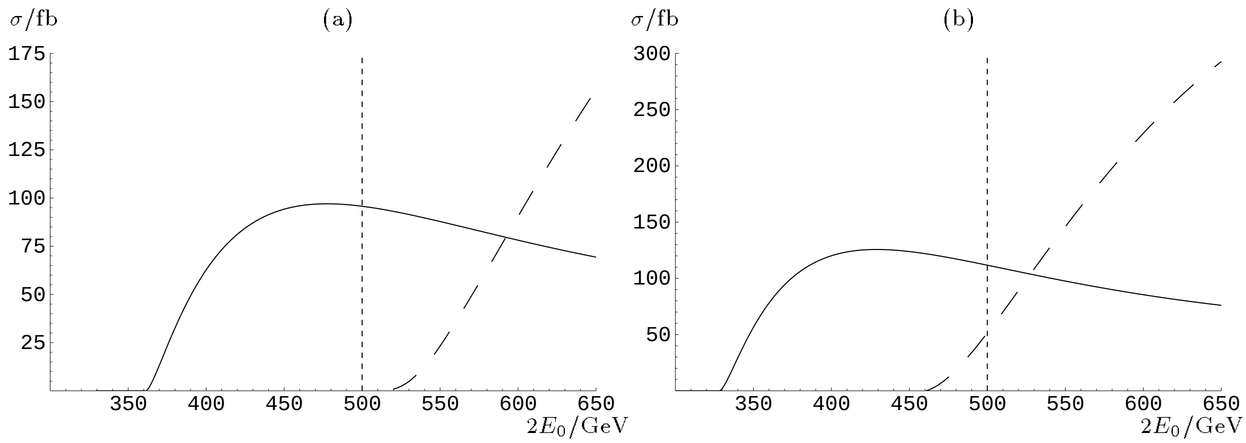

(Blöchinger, Franke, Fraas)

Extra dimensions

$\gamma\gamma \to W^+W^-$ (T.Rizzo)

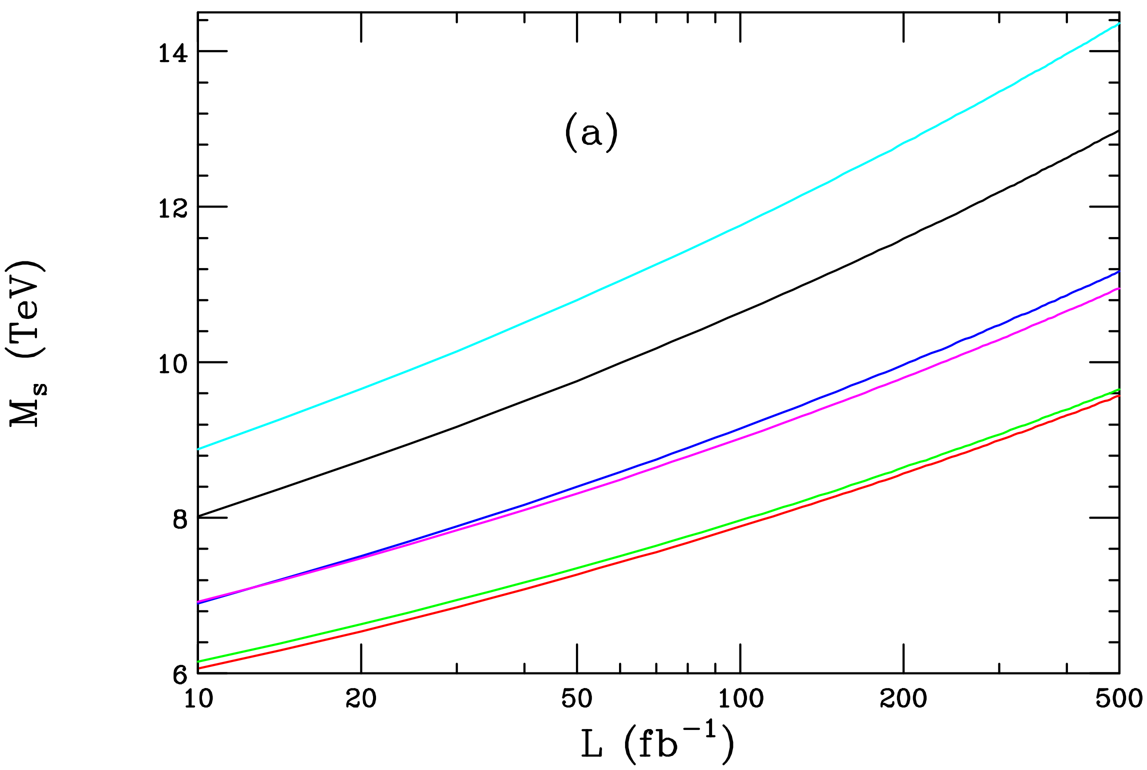

in $\gamma\gamma$: $M_s \sim (11-13)\cdot 2E_0$

in e^+e^-: $M_s \sim (6-7)\cdot 2E_0$

Anomalous gauge boson coupling

$\sigma_{\gamma\gamma \to W^+W^-} \sim 80$ pb
$\sigma_{\mathrm{e}^+\mathrm{e}^- \to W^+W^-} \sim 2$ pb (without ν exchange)

as result in $\gamma\gamma$ collisions anomaleous γWW couplings can be measured with higher accuracy, (beside $\mathrm{e}^+\mathrm{e}^-$ involves Z contribution)

$\sigma_{\gamma e \to W\nu} \propto (1 - 2\lambda_e)$

$\Rightarrow$ very sensitive to admixture of right-handed currents

Gold-plated processes at photon colliders

Reaction	Remarks
$\gamma\gamma \to h_0 \to \bar{\mathrm{b}}\mathrm{b}$	$\mathcal{SM}$ (or $\mathcal{MSSM}$) Higgs, $M_{h_0} < 160\mathrm{GeV}$
$\gamma\gamma \to h_0 \to WW(WW^*)$	$\mathcal{SM}$ Higgs, $140\mathrm{GeV} < M_{h_0} < 190\mathrm{GeV}$
$\gamma\gamma \to h_0 \to \mathrm{ZZ}(\mathrm{ZZ}^*)$	$\mathcal{SM}$ Higgs, $180\mathrm{GeV} < M_{h_0} < 350\mathrm{GeV}$
$\gamma\gamma \to H, A \to \bar{\mathrm{b}}\mathrm{b}$	$\mathcal{MSSM}$ heavy Higgs, for intermediate $\tan\beta$
$\gamma\gamma \to \tilde{f}\bar{\tilde{f}}$, $\tilde{\chi}_i^+\tilde{\chi}_i^-$, H^+H^-	large cross sections, possible observ. of FCNC
$\gamma\gamma \to S[\tilde{t}\bar{\tilde{t}}]$	$\tilde{t}\bar{\tilde{t}}$ stoponium
$\gamma\mathrm{e} \to \tilde{e}^-\tilde{\chi}_1^0$	$M_{\tilde{e}^-} < 0.9 \times 2E_0 - M_{\tilde{\chi}_1^0}$
$\gamma\gamma \to W^+W^-$	anomalous W interact., extra dimen.
$\gamma\mathrm{e}^- \to W^-\nu_e$	anomalous W couplings
$\gamma\gamma \to WW + WW(ZZ)$	strong WW scatt., quartic anom. W, Z coupl.
$\gamma\gamma \to t\bar{t}$	anomalous top quark interactions
$\gamma\mathrm{e}^- \to \bar{t}b\nu_e$	anomalous Wtb coupling
$\gamma\gamma \to$ hadrons	total $\gamma\gamma$ cross section
$\gamma\mathrm{e}^- \to e^-X$ and $\nu_e X$	structure functions (pol. and unpol.)
$\gamma g \to \bar{\mathrm{q}}\mathrm{q}$, $\bar{\mathrm{c}}\mathrm{c}$	gluon distribution in the photon
$\gamma\gamma \to J/\psi\, J/\psi$	QCD Pomeron

Electron to Photon Conversion

Spectrum of the Compton scattered photons

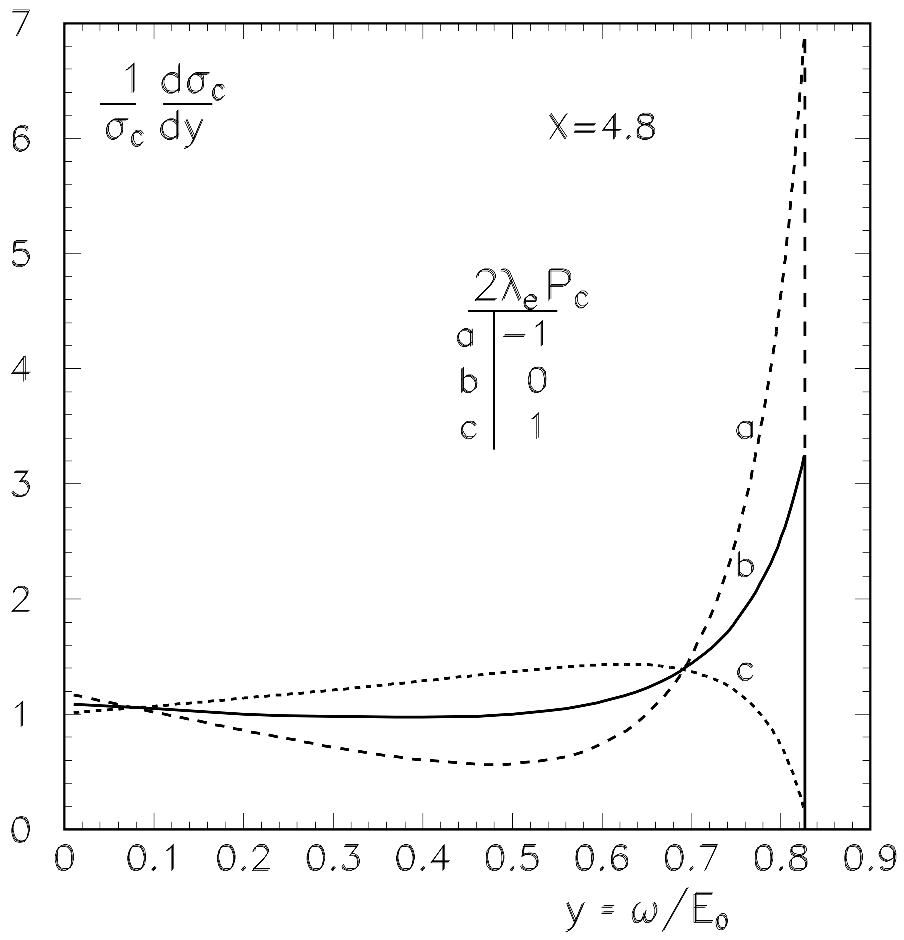

Mean helicity of the scattered photons

$x = 4.8$

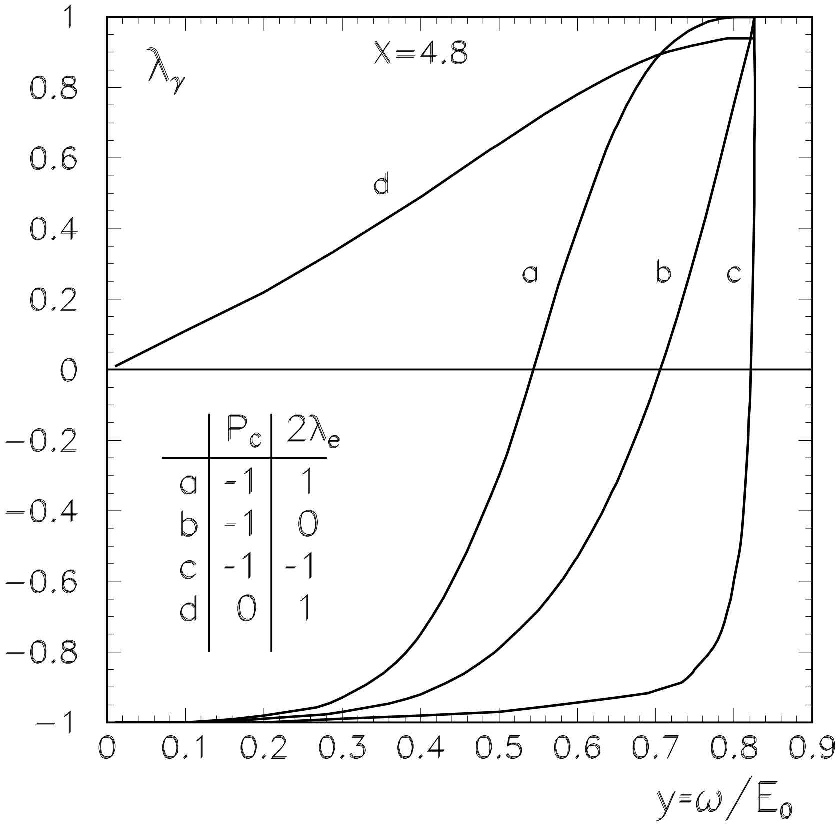

(in the case a) photons in the high energy peak have $\lambda_\gamma \approx 1$)

The cross section of the Higgs production

$$\sigma(\gamma\gamma \ \to h) \propto 1 + \lambda_1\lambda_2$$

The cross section for main backgound

$$\sigma(\gamma\gamma \ \to b\bar{b}) \propto 1 - \lambda_1\lambda_2$$

Mean photon helicity for various x and electron helicity

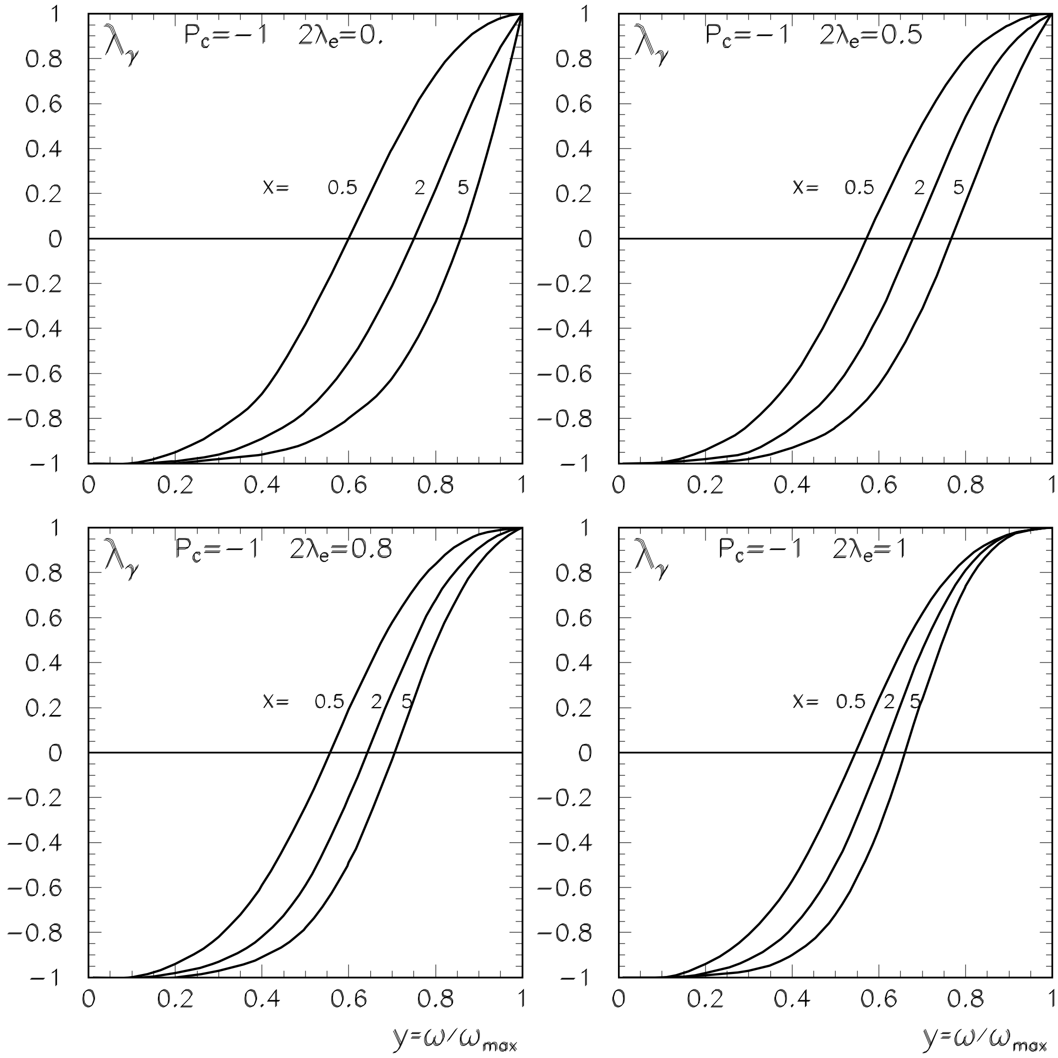

Linear polarization of the scattered photons for various x

Electrons are unpolarized and $P_l = 1$.

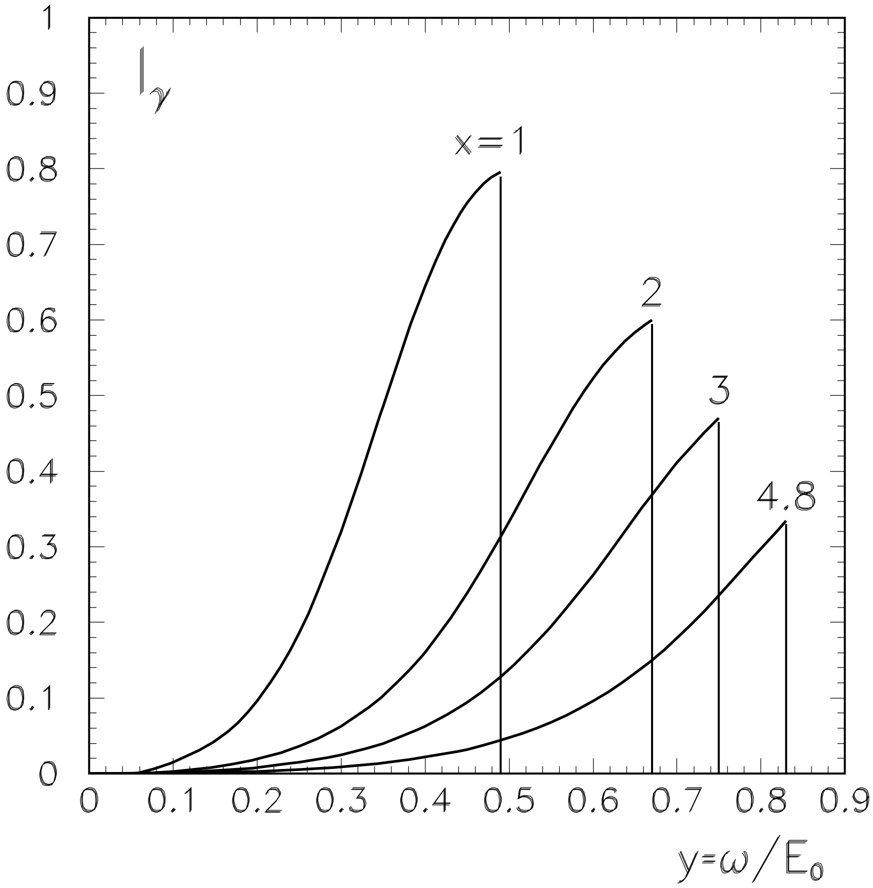

The cross section for the Higgs production

$$\sigma(\gamma\gamma \to h) \propto 1 \pm l_{\gamma,1} l_{\gamma,2}$$

For laser with $\lambda = 1.06$ μm and $M_H = 130$ GeV $x = 1.8$ and $l_\gamma = 0.63$ (high enough).

Nonlinear effects in Compton scattering

$$\xi^2 = \frac{e^2 \bar{F}^2 \hbar^2}{m^2 c^2 \omega_0^2} = \frac{2 n_\gamma r_e^2 \lambda}{\alpha}$$

Photon specta

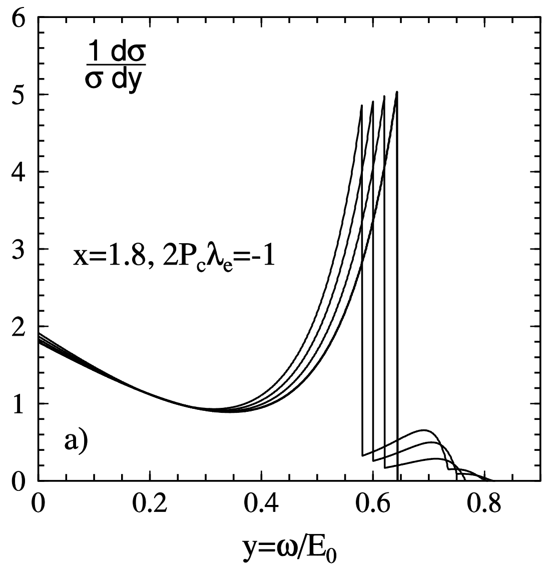

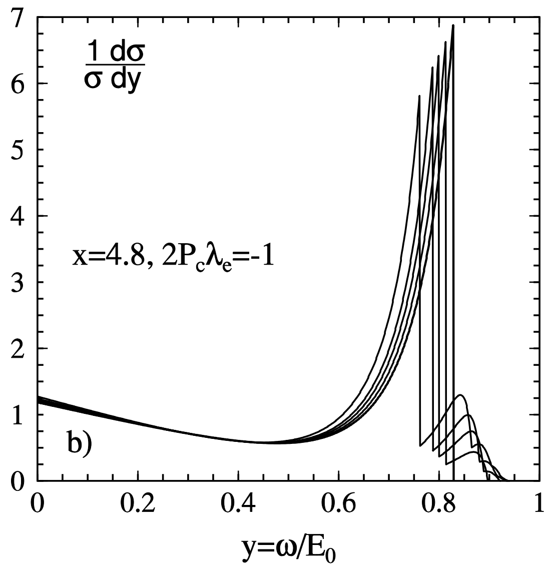

$\gamma\gamma$ luminosity spectra

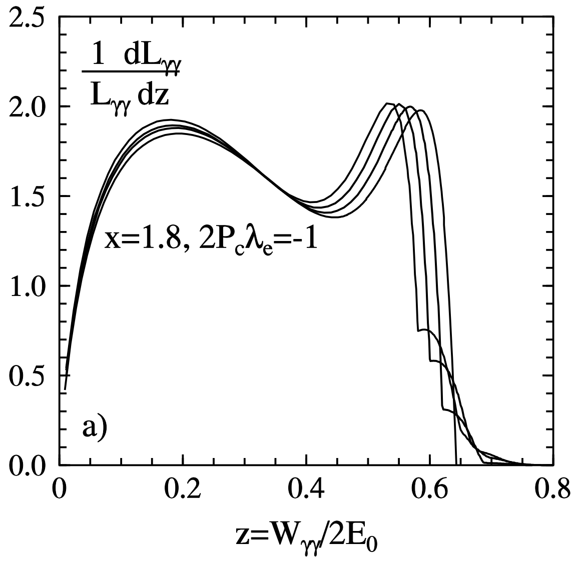

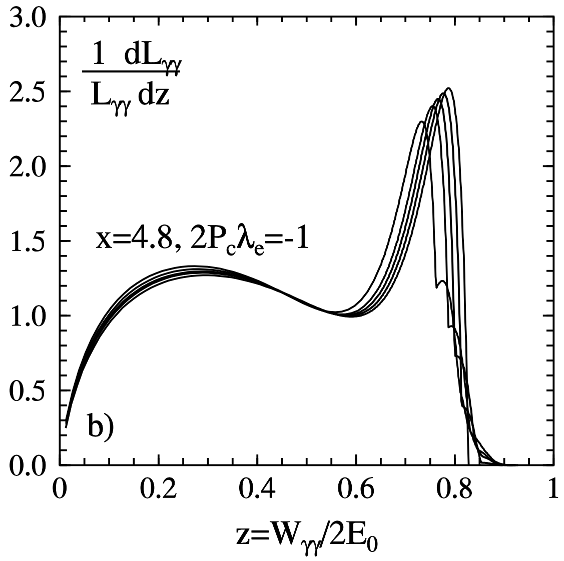

(Curves from right to left correspond to $\xi^2 = 0, 0.1, 0.2, 0.3, 0.5$)

e^+e^- pair creation in the collision of laser and high energy photons

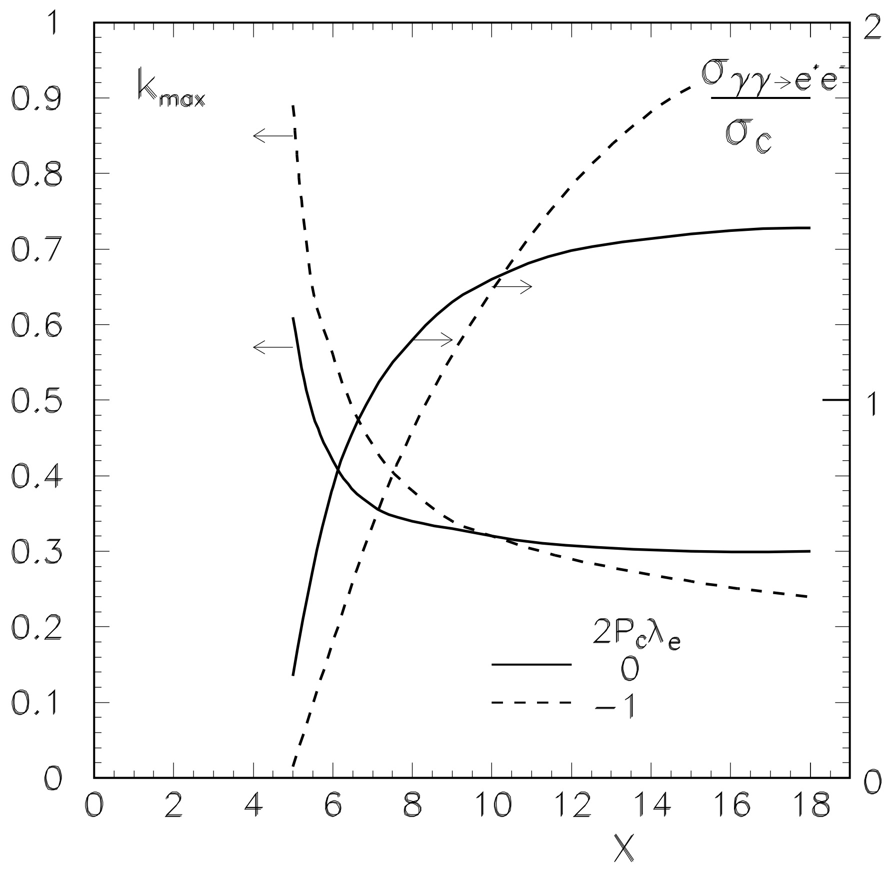

The optimum correspond to the threshold of e^+e^- creation: $x = 4.8$. Corrsponding wavelength

$$\lambda = 4.2 E_0[\text{TeV}]\,\mu\text{m}.$$

Conversion probability

In the laser focus

$$\sigma_{L,r}(z) = \sigma_{L,r}(0)\sqrt{1 + z^2/Z_R^2}$$

$$\sigma_{L,r}(0) = \sqrt{\frac{\lambda Z_R}{2\pi}}$$

R is the Rayleigh length (β–function in aceelerator terms)

For calculation of conversion probability also important: • nonlinear effects, • collisions angle, • crab-crossing angle (gives effective $\sigma_x = \sigma_z \alpha_c/2$).

Conversion probability as a function of the Rayleigh length ($x = 4.8$, $\lambda = 1.06$, $\alpha_c = 30$ mrad, optics is situated outside the electron beam)

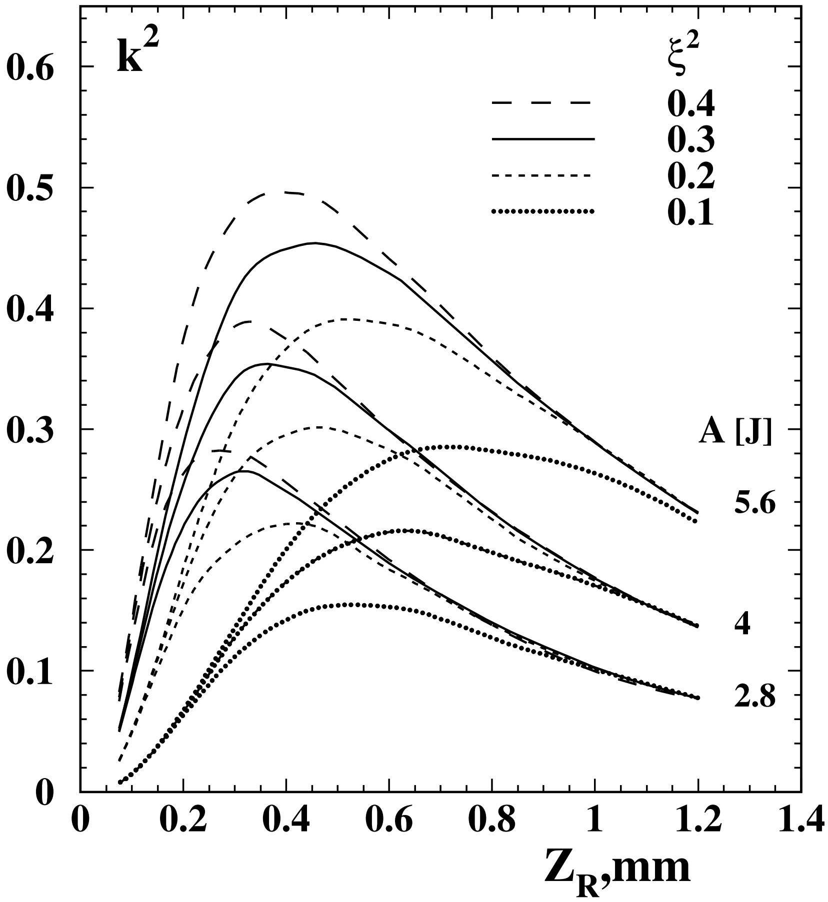

$\Rightarrow A \sim 5$ J, $Z_R \sim 0.35$ mm, $\sigma_{L,z} \sim 1.5$ ps

The Interaction Region

Collisions effects

Coherent pair creation
Beamstrahlung
Beam-beam repulsion
Depolarization (not important)

Dependence of $\gamma\gamma$ and γe luminosities in the high energy peak on the horizontal beam size

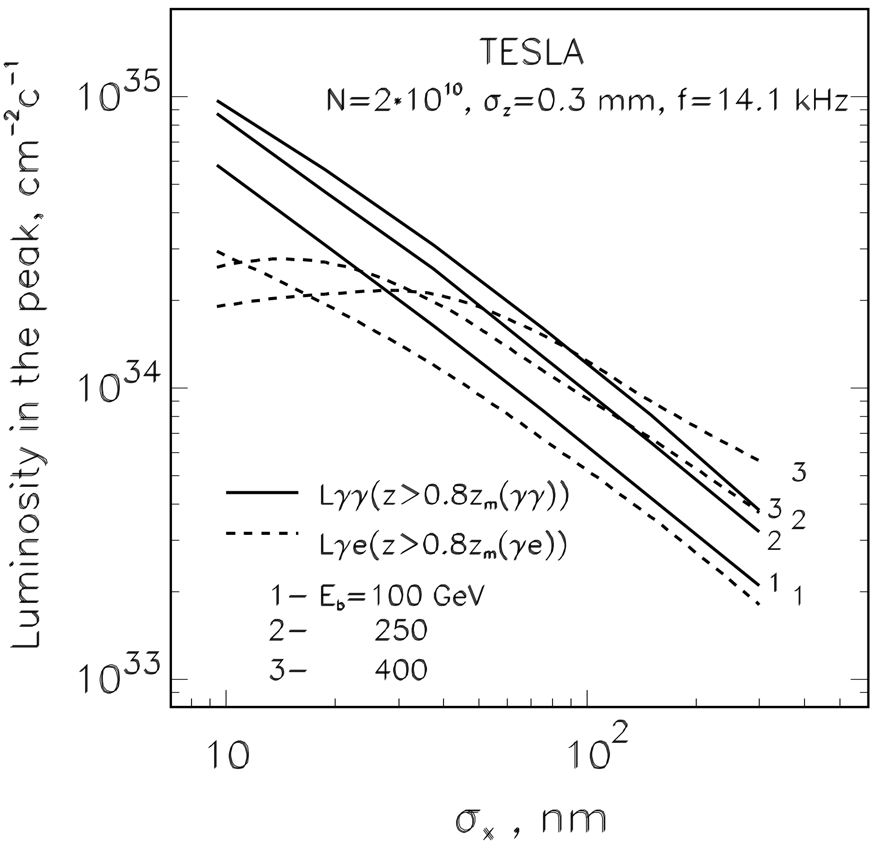

For the TESLA electron beams $\sigma_x \sim 100$ nm at $2E_0 = 500$. Having beams with smaller emittances one could have by one order higher $\gamma\gamma$ luminosity.

γe luminosity in the high energy peak is limited due to the beam repulsion and beamstrahlung

Maximum disruption angles

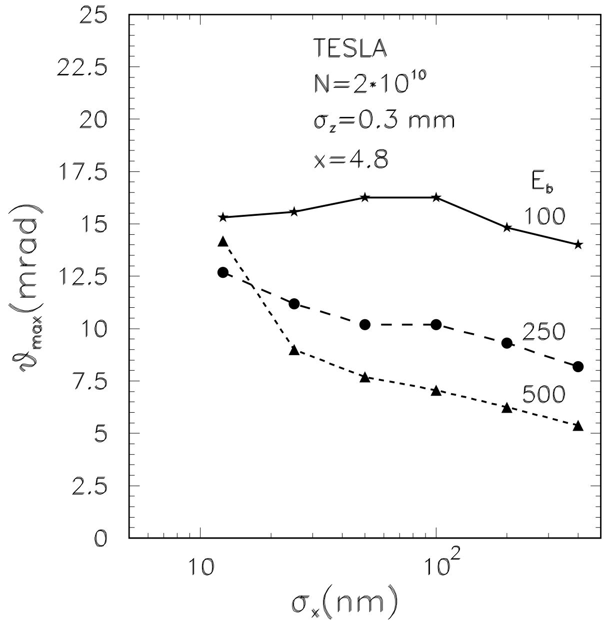

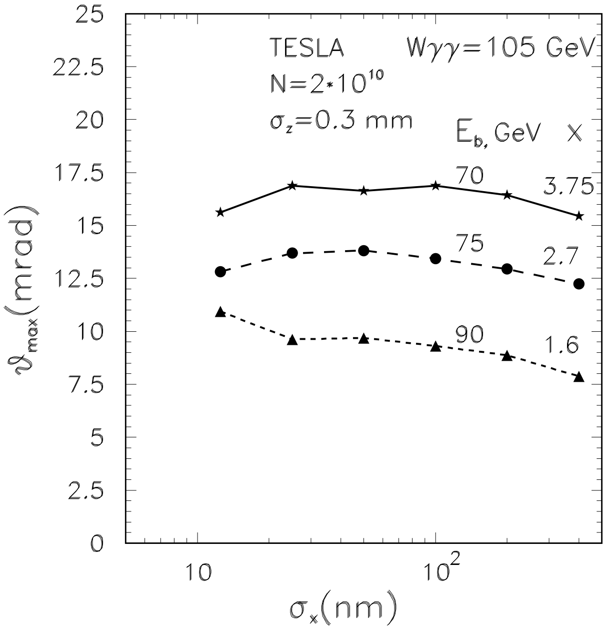

$$\vartheta \propto \frac{x}{\sqrt{(x+1)\sigma_c(x)}}$$

Chromo-geometric aberrations in the final focus system

Dependence of the geometric e^-e^- luminosity on the horizontal β-function (SLAC design).

For TESLA the $\sigma_E/E \sim 10^{-3}$ (σ_E in the figure)

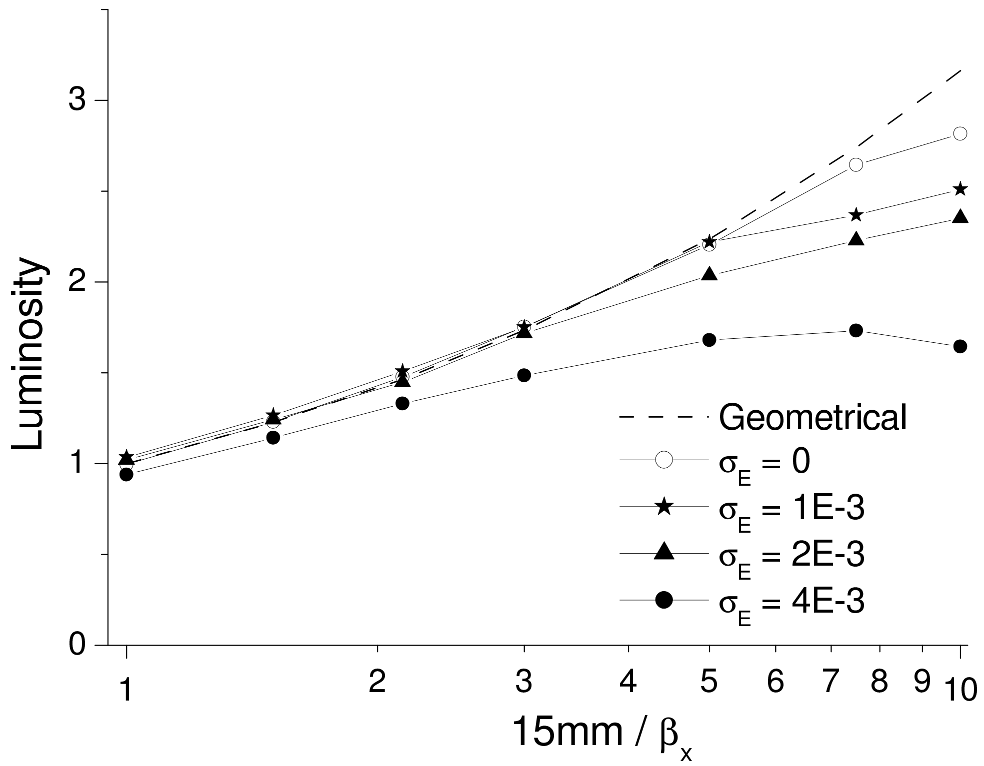

$\gamma\gamma$ and γe luminosities at TESLA

Summary table

$2E_0$ GeV	200	500	800
λ_L [μm]/x	1.06/1.8	1.06/4.5	1.06/7.2
t_L [λ_{scat}]	1.35	1	1
$N/10^{10}$	2	2	2
σ_z [mm]	0.3	0.3	0.3
$f_{rep} \times n_b$ [kHz]	14.1	14.1	14.1
$\gamma\epsilon_{x/y}/10^{-6}$ [m·rad]	2.5/0.03	2.5/0.03	2.5/0.03
$\beta_{x/y}$ [mm] at IP	1.5/0.3	1.5/0.3	1.5/0.3
$\sigma_{x/y}$ [nm]	140/6.8	88/4.3	69/3.4
b [mm]	2.6	2.1	2.7
L_{ee}(geom) [10^{34}]	4.8	12	19
$L_{\gamma\gamma}(z > 0.8 z_{m,\gamma\gamma})[10^{34}]$	0.43	1.1	1.7
$L_{\gamma e}(z > 0.8 z_{m,\gamma \mathrm{e}})[10^{34}]$	0.36	0.94	1.3
$L_{ee}(z > 0.65)[10^{34}]$	0.03	0.07	0.095

For the same energy and TESLA beams

$$L_{\gamma\gamma}(z > 0.8 z_m) \approx \frac{1}{3} L_{\mathrm{e^+e^-}}$$

(however cross sections in $\gamma\gamma$ collisions are typicaly larger the in e$^+$e$^-$ by one order of magnitude)

More universal relation (for $k^2 = 0.4$)

$$L_{\gamma\gamma}(z > 0.8 z_m) \approx 0.1 L_{ee}(geom)$$

$\gamma\gamma$ luminosity spectra

with various cuts on the longitudinal momentum; 0 and 2 are the total helicities of colliding photons

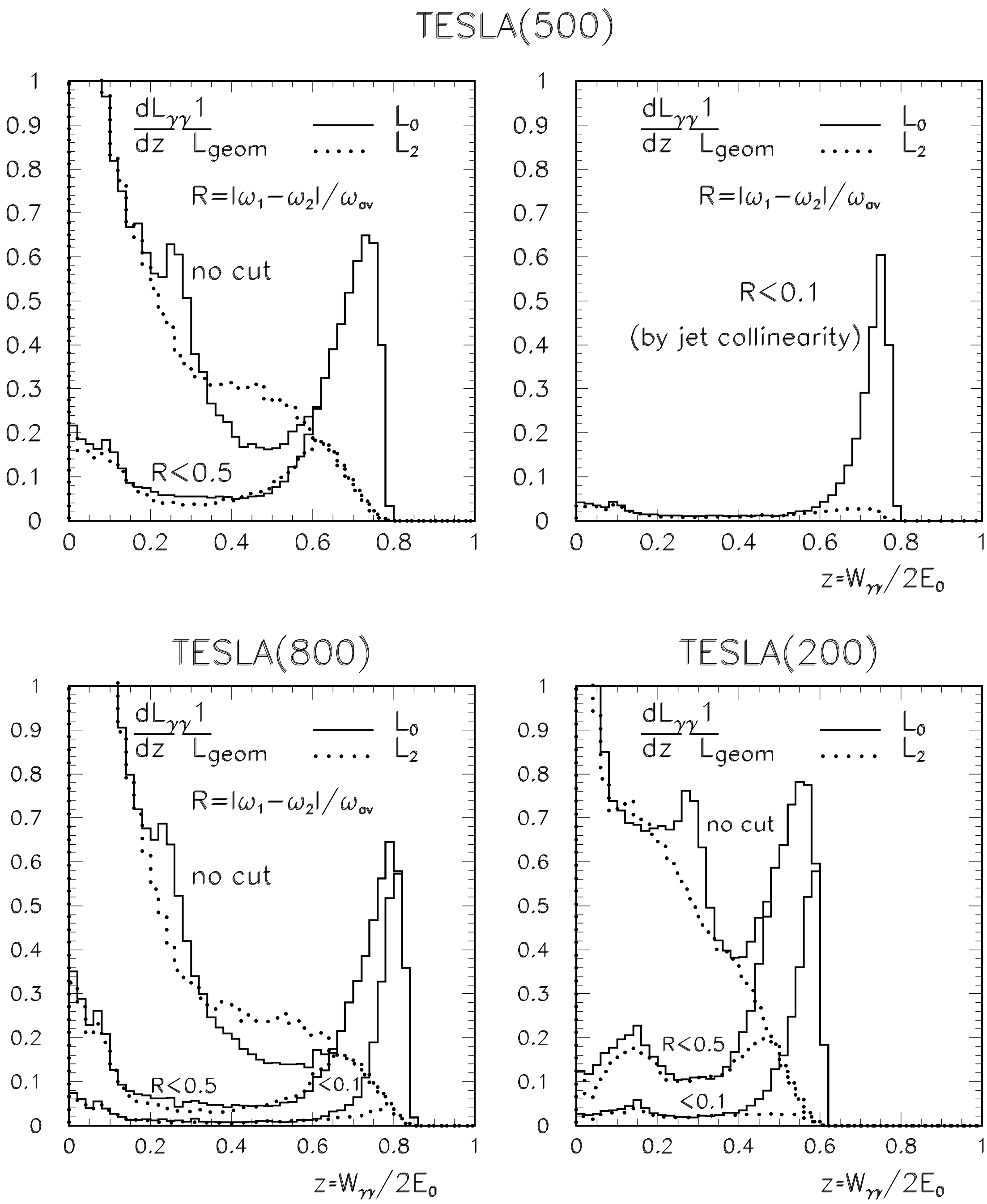

γe luminosity spectra

($\gamma\gamma$ collisions are optimized, γe conversions for both beams, $b = 2.1$ mm)

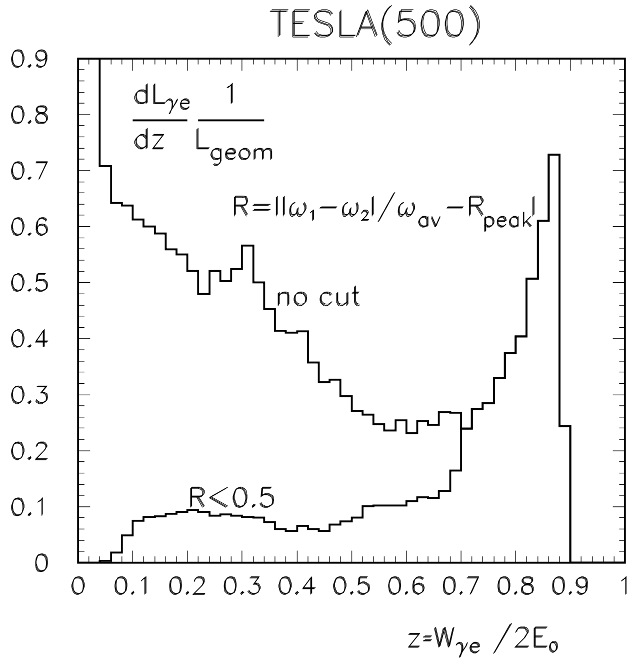

(γe collisions are optimized, γe conversions for one beams, $b = 1.7$ cm)

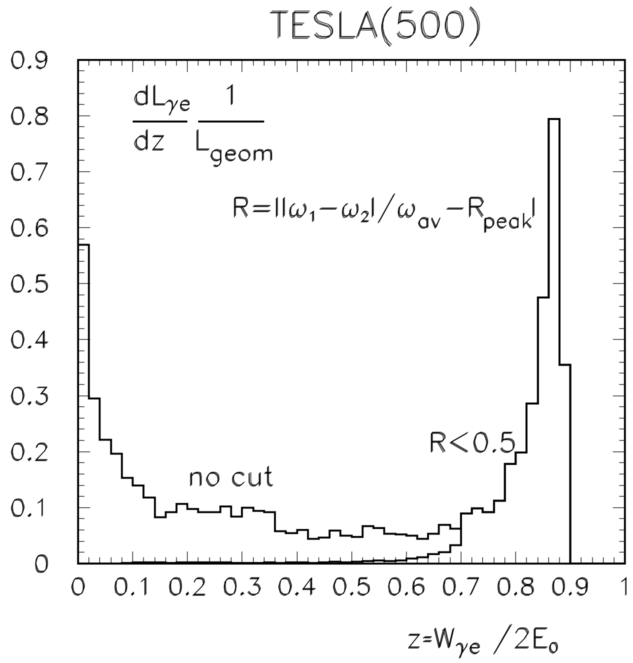

Luminosity measurement

$\gamma\gamma$ collisions The luminosity is a function of the invariant mass $W_{\gamma\gamma} = \sqrt{4\omega_1\omega_2}$ and rapidity $\eta = 0.5 \ln(\omega_1/\omega_2)$. Also polarization should be measured.

In other words, one should measure the spectral luminosities $dL_0/dW_{\gamma\gamma}d\eta$ and $dL_2/dW_{\gamma\gamma}d\eta$ with the total helicity 0 and 2.

The process $\gamma\gamma \to l^+l^-$, where $l = e$ or μ is the best.

$$\sigma_0(|\cos\vartheta| < a) \approx \frac{4\pi\alpha^2}{W_{\gamma\gamma}^2}\frac{8m^2}{W_{\gamma\gamma}^2}\left[\frac{1}{2}\ln\left(\frac{1+a}{1-a}\right) + \frac{a}{1-a^2}\right]$$

$$\sigma_2(|\cos\vartheta| < a) \approx \frac{4\pi\alpha^2}{W_{\gamma\gamma}^2}\left[2\ln\left(\frac{1+a}{1-a}\right) - 2a\right].$$

One can see that $\sigma_0/\sigma_2 \sim m^2/W_{\gamma\gamma}^2 \ll 1$ (excluding the region of small angles). For photons with arbitrary circular polarizations the cross section is

$$\sigma_{\gamma\gamma\to e^+e^-} = \frac{1+\lambda_1\lambda_2}{2}\sigma_0 + \frac{1-\lambda_1\lambda_2}{2}\sigma_2,$$

where $\sigma_2 \gg \sigma_0$.

Hence the number of events

$$dN_{\gamma\gamma\to\mu^+\mu^-} \approx dL\,\frac{1-\lambda_1\lambda_2}{2}\,\sigma_2 \equiv dL_2\,\sigma_2\,,$$

and one can measure the luminosity $dL_2/dW_{\gamma\gamma}d\eta$. Measurement of $dL_0/dW_{\gamma\gamma}d\eta$ is done by inversion of the helicity of one photon beam simultaneously changing the signs of the helicities of the laser beam used for the $e \to \gamma$ conversion and that of the electron beam.

Measurement of linear polarization in $\gamma\gamma$ collisions

At high energy and not too small angles the cross section is

$$d\sigma = \frac{\alpha^2}{W_{\gamma\gamma}^2}\left[(1-\lambda_1\lambda_2)\left(\frac{W_{\gamma\gamma}^2}{\mathbf{p}_{-\perp}^2}-2\right) - 2l_1\, l_2\cos(2\phi_1+2\phi_2)\right] d\Gamma\,,$$

$$d\Gamma = \frac{2\omega_1\omega_2}{[\omega_1(1-\cos\theta_-)+\omega_2(1+\cos\theta_-)]^2}\, d\Omega_-$$

where $W_{\gamma\gamma}^2 \gg m^2$, $\quad \mathbf{p}_{-\perp}^2 \gg m^2$, $\phi_i = \varphi_- - \gamma_i$ is the (azimuthal) angle between the vector $\mathbf{p}_{-\perp}$ and the direction of the linear polarization of i-th photon.

One sees that at large angles ($p_\perp \sim W_{\gamma\gamma}/2$) the cross section depends strongly on the degrees of both the circular and the linear photon polarizations.

Measurement of luminosity in γe collisions

In this case the total cross section

$$\sigma \approx (1 + 2\lambda_e\lambda_\gamma)\,\frac{2\pi\alpha^2}{W_{\gamma \mathrm{e}}^2}\,\ln\frac{W_{\gamma \mathrm{e}}^2}{m^2}, \qquad W_{\gamma \mathrm{e}}^2 \gg m^2$$

depends only on circular polarization.

The differential cross section depends on circular and linear polarizations

$$d\sigma = \frac{\alpha^2\,F_0}{m^2 x}\,d\Gamma\,, \quad d\Gamma = \delta(p + k - p' - p')\frac{d^3p'd^3k'}{E'\omega'} = dyd\varphi_\gamma$$

where

$$x = \frac{2pk}{m^2} \approx \frac{4E\omega}{m^2} \gg 1\,, \quad y = 1 - \frac{pk'}{pk}, \quad r = \frac{y}{(1-y)x}$$

φ_γ is the azimuthal angle of the final photon, F_0 is

$$F_0 = \frac{1}{1-y} + 1 - y - 4r(1-r)\left[1 + l_\gamma\,\cos 2(\varphi - \gamma)\right] -$$

$$-y\lambda_\gamma\left[2\sqrt{r(1-r)}\,\zeta_\perp\,\cos(\varphi - \beta) - \frac{2-y}{1-y}(1-2r)\,2\lambda_e\right].$$

In the region of angles $\theta_\gamma \gg m/E$, we have

$$1 - y = \frac{E(1-\cos\theta_\gamma)}{E(1-\cos\theta_\gamma) + \omega(1+\cos\theta_\gamma)}$$

$$d\Gamma = \frac{2E\omega}{[E(1-\cos\theta_\gamma) + \omega(1+\cos\theta_\gamma)]^2}\,d\Omega_\gamma\,.$$

If the angle $\theta_\gamma \approx 1$ all terms have to be taken into account. Thus by detecting the final state particles at large angles, one can measure all polarization parameters of the colliding particles.

Backgrounds at photon colliders.

1. Disrupted beams.

2. Electron-positron pairs.

3. Large angle Compton scatterings.

4. Large angle beamstrahlung.

5. SR from halo particles.

6. $\gamma\gamma \rightarrow$ hadrons.

1) Disrupted beams.

Low energy electrons after multiple Compton scattering and coherent pair creation are deflected on opposing electron beam. The maximum disruption angles are about 10 mrad. These particles should be removed from the detector without any interactions. Solution - the crab crossing, $\alpha_c \approx 30$ mrad (34 mrad at TESLA).

2) Electron-positron pairs.

a) $\gamma\gamma \to e^+e^-$, b) $\gamma e \to e + e^+e^-$, c) $ee \to ee + e^+e^-$.
Situation is approximately similar to that in e^+e^- collisions. There are

- unavoidable hard large angle particles with acceptable rate;
- many low P_t due to kick on the opposing electron beam. Due to solenoidal magnetic field these particles are confined in the region

$$r^2 < 0.12 \frac{N}{10^{10}} \frac{z[\mathrm{cm}]}{\sigma_z[\mathrm{mm}] B[\mathrm{T}]}$$

Vacuum pipe should be at larger distance.

3) Large angle Compton scatterings.

$$\omega = 4\omega_0/\vartheta^2 \qquad \text{at} \qquad \vartheta \gg 1/\gamma$$

– no problem for the detector, question only for the mirrors ($\omega \sim 40$ keV at $\vartheta = 10$ mrad (the edge of the mirror)).
Density of radiation at the distance L

$$dn/ds \propto N/\gamma^2 L^2 \vartheta^4$$

Result of simulation for $2E_0 = 500$ GeV:

$$P \sim 10^{-7} \quad \mathrm{W/cm^2}, \;\; \omega \sim 40 \;\; \mathrm{keV} \quad \text{at} \quad \vartheta = 10 \; \mathrm{mrad}.$$

4) Large angle beamstrahlung.

Full beam collision simulation gives: X-ray photons have wide spectrum

$$P \sim 10^{-6} \quad \mathrm{W/cm^2}, \ \bar{\omega} \sim 1.5 \ \mathrm{keV} \quad \mathrm{at} \quad \vartheta = 10 \ \mathrm{mrad}.$$

X-rays (items 3-4) may course radiation damage problem for dielectric mirrors, this question was not studied yet. Ionized residual gas can also produce carbon deposits on mirrors (was observed at storage ring).

5) SR halo particles.

It is supposed that electron beams are collimated so that the cone of X-ray radiation produced in the final focus system does not hit opposing final quad. This problem exist for e^+e^- as well.
At photon colliders with crab crossing and open angle ± 10 mrad for disrupted beams it should be no problem. Some worries exist about new halo, arising after collimation.

6) $\gamma\gamma \to$ hadrons.

$\sigma_{tot} \sim 500$ nb^{-1}

For TESLA at $2E_0 = 500$ GeV and expected luminosities the "effective number" (with $W_{\gamma\gamma} \sim 400$ GeV) of hadronic events is about 1.5 per bunch crossing.

This may cause some problems for events with jets at small angles. Below are some figures with characteristics of the hadronic background.

Distribution of particle flow (left) and energy flow (right) in pseudo-rapidity for various values of $W_{\gamma\gamma}$ assuming equal energies photons)

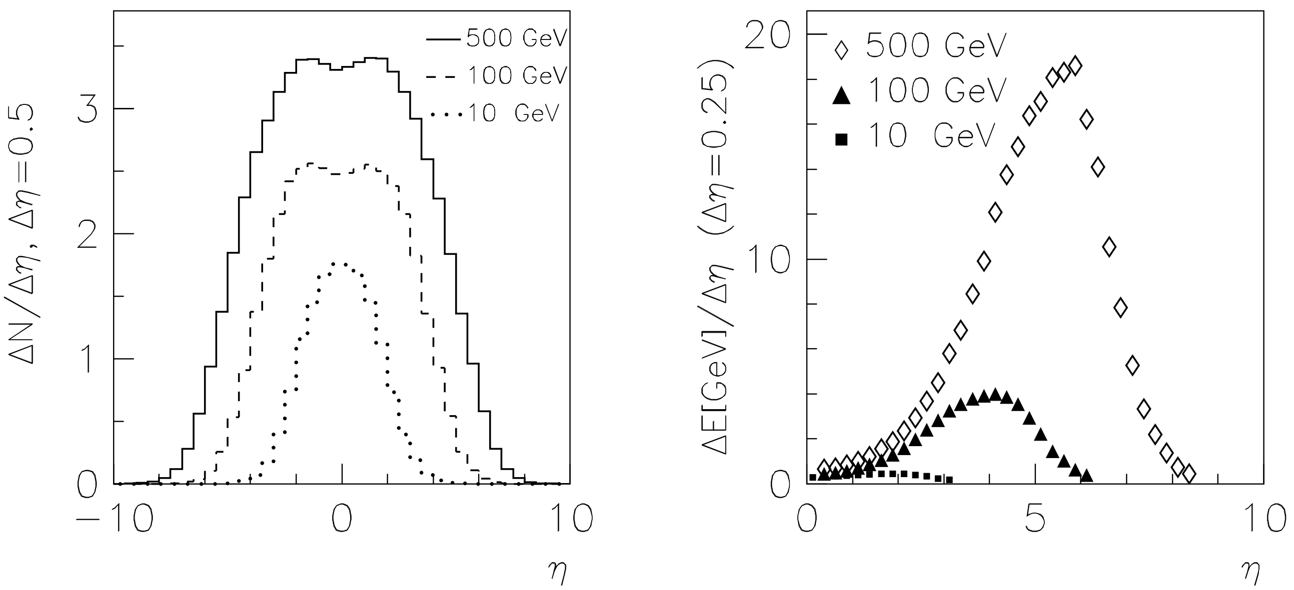

Distribution of particles in pseudo-rapidity for different ranges of $\gamma\gamma$ invariant mass.

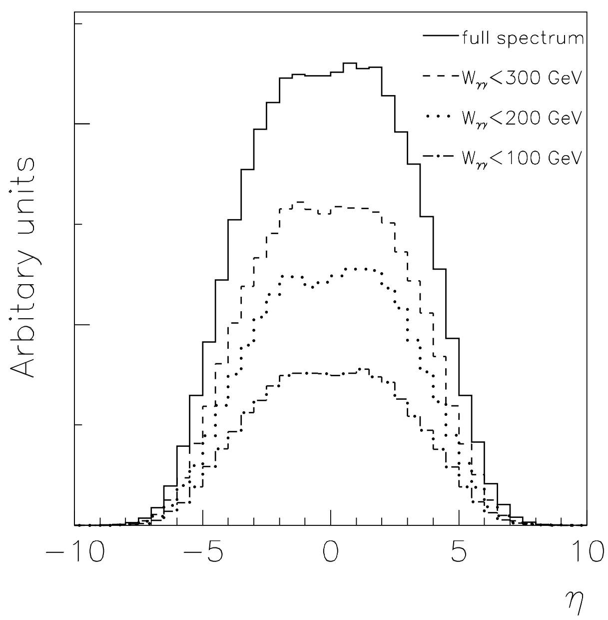

The probability of an energy deposition in the detector above the value E due to the process $\gamma\gamma \to hadrons$. Curves a), b), c) correspond to 7, 2 and 0.7 hadronic events on the average per beam collision respectively.

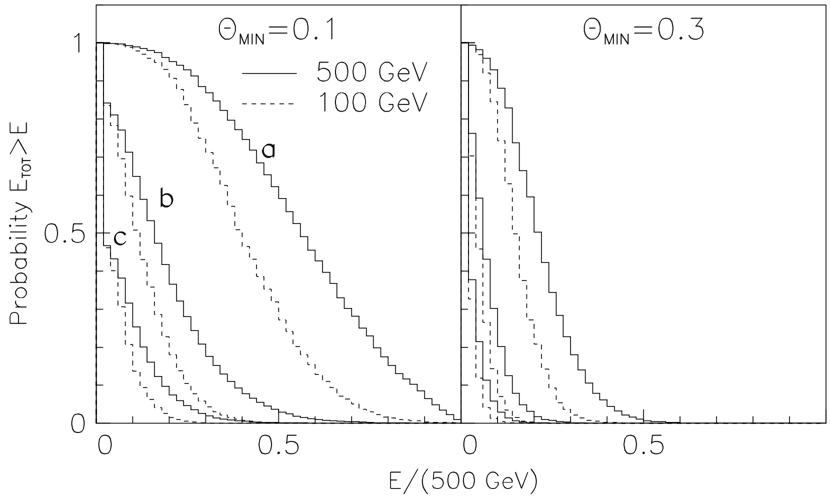

The probability to find an unbalanced transverse momentum above some p_t. Curves correspond to 7, 2, 0.7 $\gamma\gamma \to hadrons$ events on the average per beam collision.

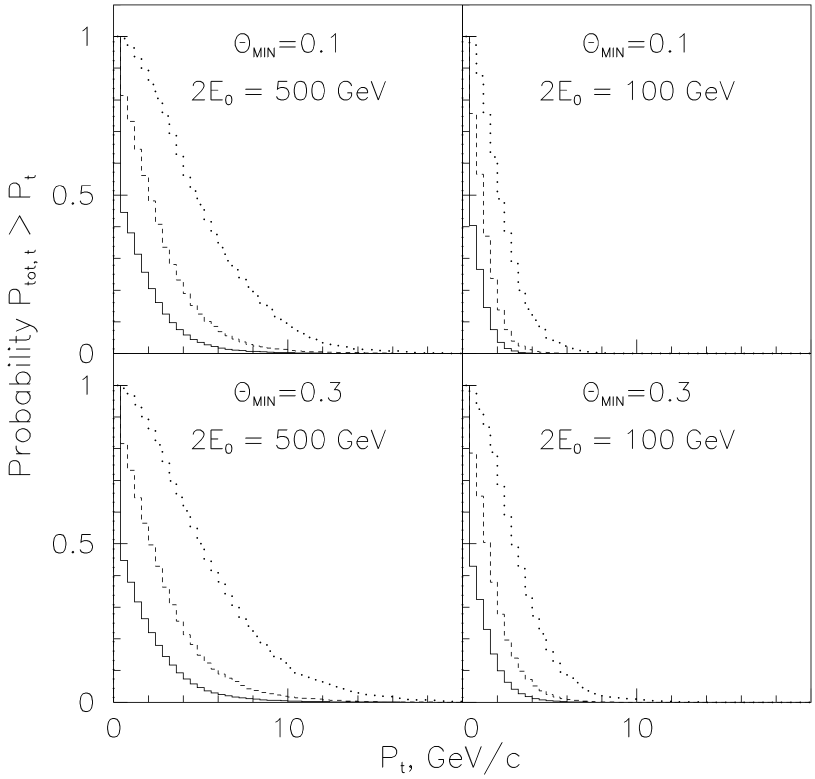

The probability to have the energy flow into $\Delta\phi \times \Delta\eta =$ 0.3×0.3 cell above some threshold (abscissa value) for 4 pseudo-rapidity points: η =0, 1, 2, 3. $W_{\gamma\gamma}$ is 500 GeV (left) and 100 GeV (right).

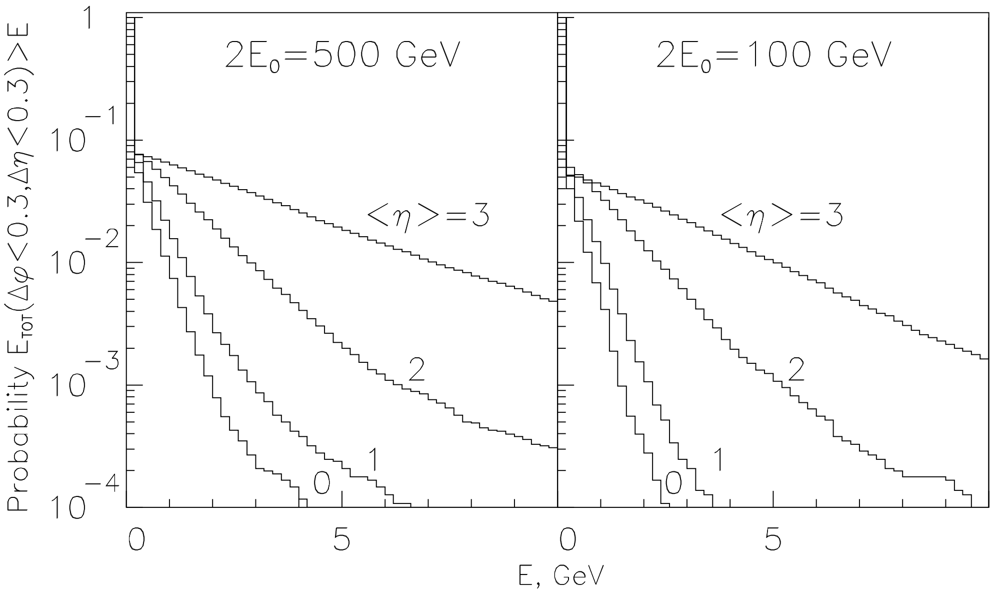

For "central" events the jet size is just $\Delta\Omega$. Due to the relation $d\Omega = d\varphi d\eta \sin^2\vartheta$ the probability of background given in above figure should be divided by a factor of $\sin^2\vartheta$.

For the $H(115) \to \bar{b}b$ decay the optimum angular cut is $\cos\vartheta = 0.7$. For such an angle the probability of 2 GeV energy deposition inside a jet from the Higgs decay is 1.5% and thus does not present a problem even for a 10 times larger luminosity.

However, the probability depends very strongly on the angle. For example, for $\eta = 2$ the probability of 2 GeV is already 60%. So, at low angles the hadronic background can worsen the resolution for low energy jets.

This is only estimate, realistic analyses is required.

Laser and optics.

Summary of Requirements to the Laser

Flash energy	≈ 5 J
Duration	$\tau(rms) \approx 1.5$ ps
Repetition rate	TESLA collision rate, ≈ 14 kHz
Average power	≈ 140 kW (for one pass collision)
Wavelength	≈ 1 μm(for all energies).

Too large average power

multiple use of the same laser pulse is required.

The Optical Trap.

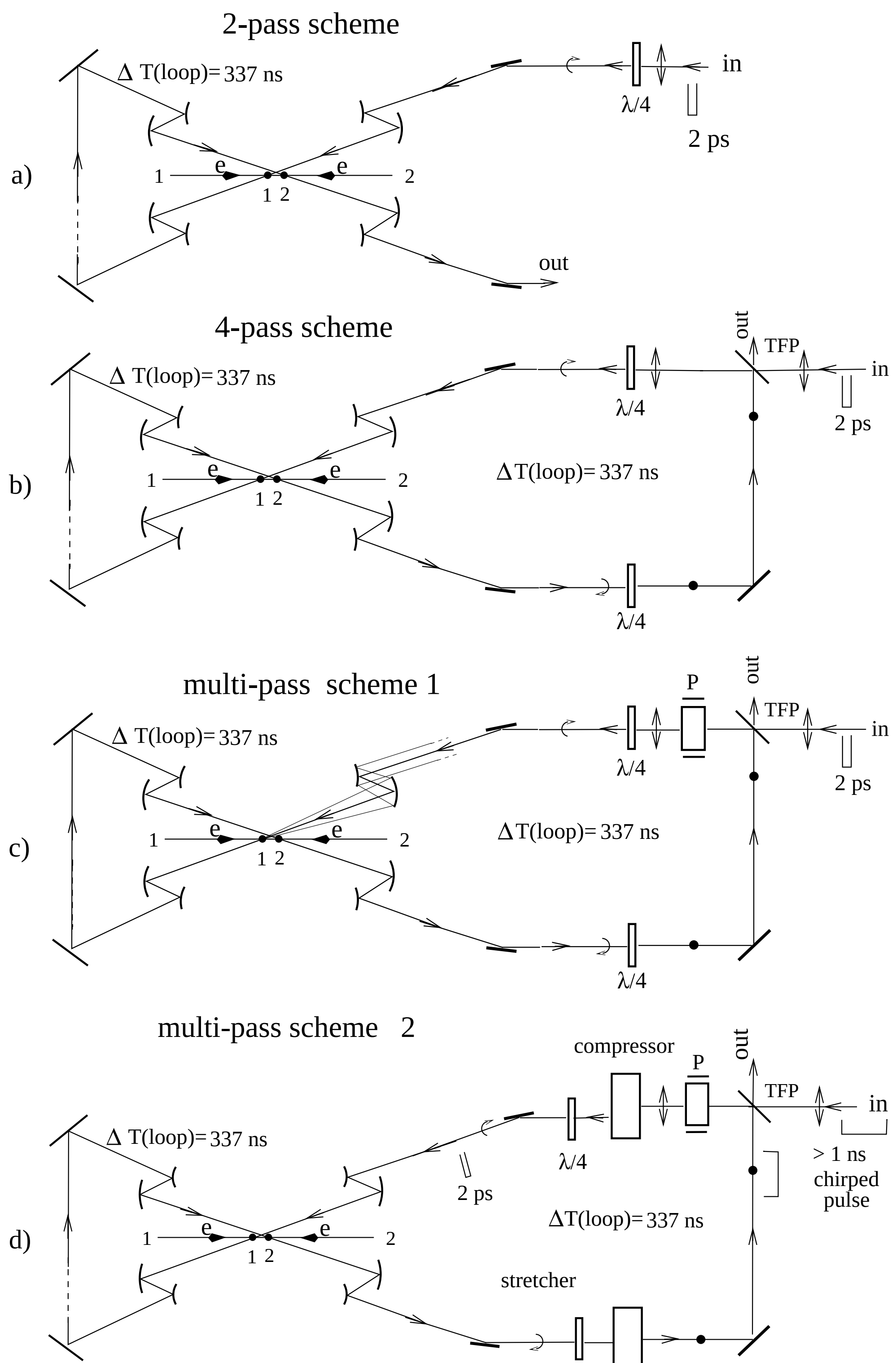

The scheme c) is the best, allows about 6 round trips (12 collisions with electron bunches). Nonlinear effects in optical elements is the main problem, but can be solved.

Merging of pulses from several lasers (amplifiers)

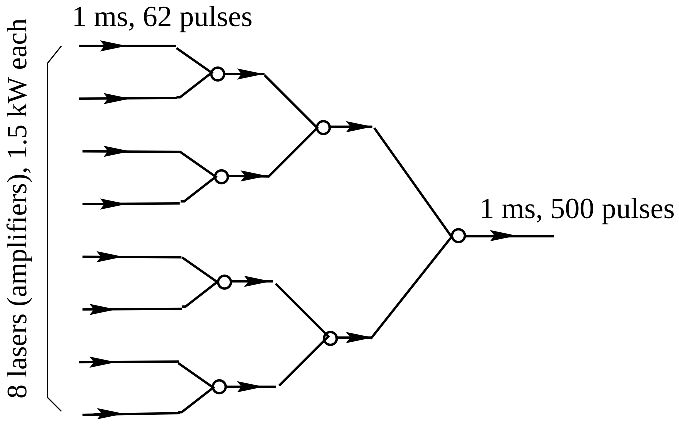

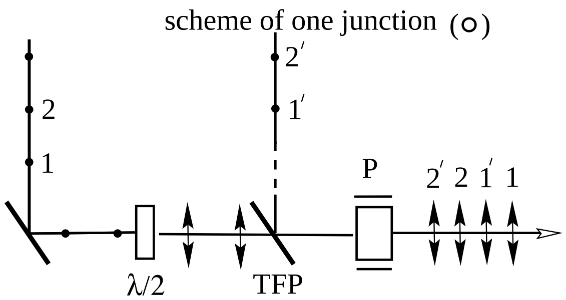

For the 6 round trip scheme

$$P_{diode} = \frac{A(\text{flash})N(\text{bunches})}{\epsilon T_0} = \frac{5\text{J} \times 500}{0.5 \times 10^{-3}} = 5\text{MW}.$$

The present cost of diodes is about 5\$/Watt

$\Rightarrow$ the cost is about 25 M\$.

Laser fusion program needs considerable reduction of the diode cost (down to 0.1\$/Watt), so the the diode cost is not a serious problem for photon colliders. The average output power of all lasers in the considered scheme is about 12 kW, or 1.5 kW for each laser.

“External” optical cavity

$$P_{cavity} = Q P_{laser}$$
$$Q \sim 50$$

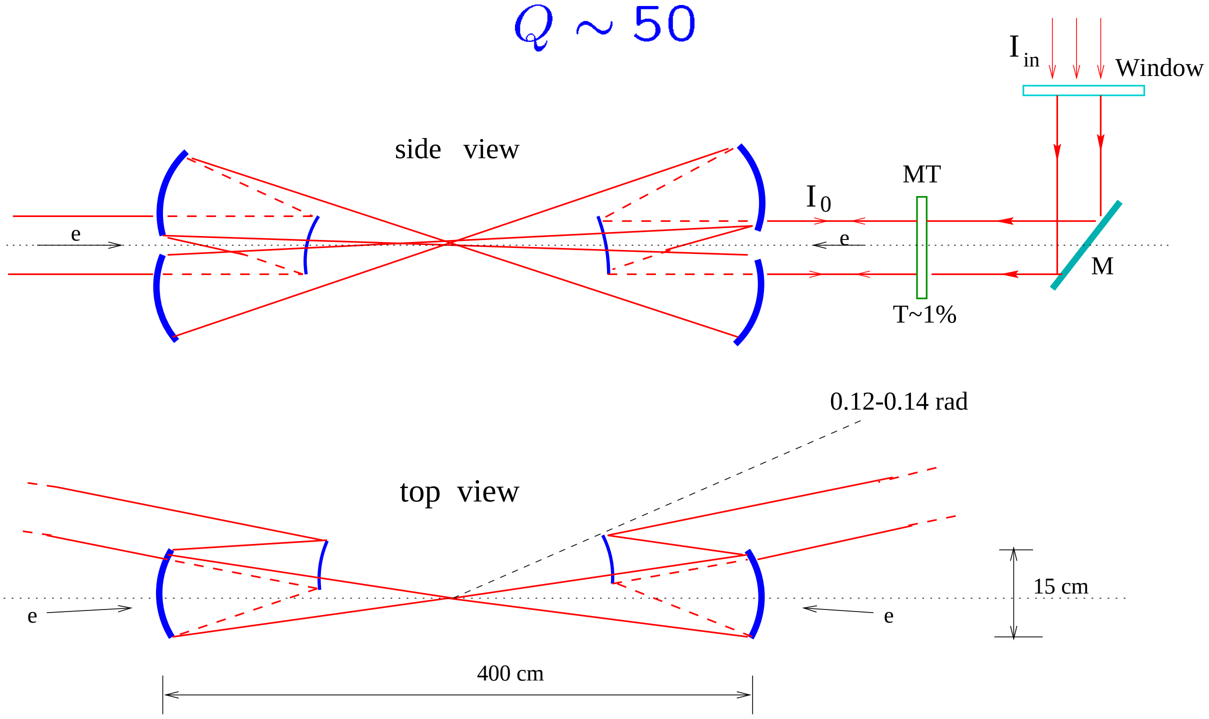

Ring type optical cavity

ring-cavity optics for e to γ conversion of one electron beam

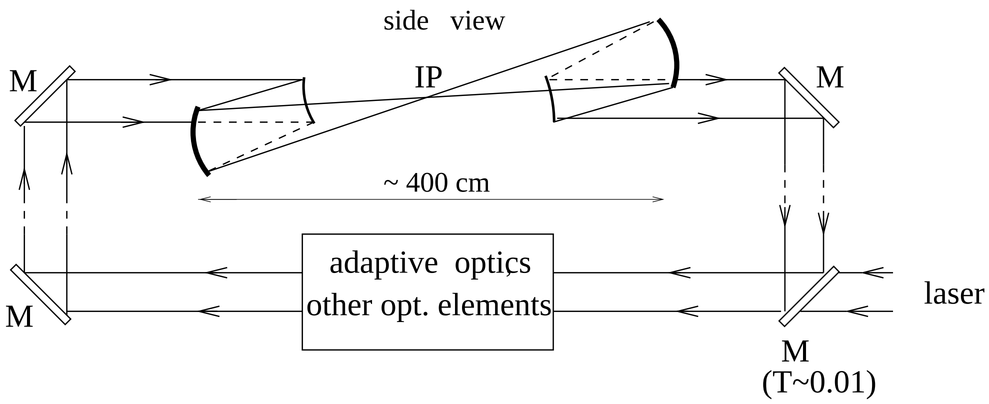

The scheme requires very small tolerances:
$$\Delta_L \sim \lambda/(2\pi Q)$$

Free-electron laser

(Saldin, Schneidmiller, Yurkov)

The FEL scheme: master oscillator–power amplifier (MOPA) scheme where the low–power radiation from a Nd glass laser ($\lambda = 1\ \mu$m) is amplified in a long tapered undulator by an electron beam

Summary on lasers

Solid state laser with the optical trap is the most attractive approach for TESLA

Conclusion

The Photon Collider presents a unique opportunity to study $\gamma\gamma$ and γe interactions at high energies and luminosities, which can considerably enrich the physics program of the e^+e^- linear collider TESLA.

This novel option requires only one new additional element: the powerful laser, which can be built using modern laser technologies. The optimum laser wave length for TESLA is about 1 μm, which is exactly the region of the most powerful developed solid state lasers.

The second interaction region and the detector may be very similar to those for e^+e^- collisions and can be also be used for study of e^-e^- or e^+e^- interactions.

The second interaction region for $\gamma\gamma$ and γe collisions is considered in the TESLA design and the special accelerator requirements are taken into account.

The next step: 2–3 year for R&D on the laser system and design of the second interaction region.